Approximating Spheroid Inductive Responses Using Spheres

J Torquil Smith and H Frank Morrison

Lawrence Berkeley National Laboratory
Berkeley, California 94720

ABSTRACT

The response of high permeability ($\mu_r \geq 50$) conductive spheroids of moderate aspect ratios (0.25 to 4) to excitation by uniform magnetic fields in the axial or transverse directions is approximated by the response of spheres of appropriate diameters, of the same conductivity and permeability, with magnitude rescaled based on the differing volumes, D.C. magnetizations, and high frequency limit responses of the spheres and modelled spheroids.

INTRODUCTION

Spheroid responses are important as limiting cases for modelling inductive responses of isolated metallic objects such as unexploded military ordnance (UXO). Full solutions for low frequency inductive responses of magnetic (permeable) conducting spheroids have recently been published together with a high frequency solution resulting from an impedance like surface condition (Ao *et al.*, 2001). While these solutions will undoubtably prove very useful, their necessarily complicated derivations are somewhat opaque to intuitive understanding of the resultant responses. Here we present a simple empirical approximation of axial and transverse responses of magnetic conducting spheroids based on the responses of spheres of the axial and transverse diameters and an intermediate diameter. Agreement is good for relative permeabilities over 50, and aspect ratios up to 4, that is, for the great majority of UXO.

APPROXIMATION

In considering approximation of spheroid responses using spheres, there are two obvious diameter spheres to try, namely spheres of the transverse spheroid diameter ($2a$), and spheres of the axial spheroid diameter ($2b$). This first suggests approximating the axial and transverse responses of a spheroid $m_z(\zeta)$ and $m_t(\zeta)$ by sphere responses $m_{sphere(b)}(\zeta)$ and $m_{sphere(a)}(\zeta)$, where ζ is either t or ω depending on whether a time domain or frequency domain response is being approximated. However given the differences in magnetization and volume between spheroids and spheres, one would not expect amplitudes to agree without some rescaling.

The low frequency limit polarizability of a permeable spheroid of relative permeability μ_r is readily calculable, both for axial external magnetic fields [$m_z(\omega{=}0)$] and for transverse magnetic fields [$m_t(\omega{=}0)$] (see Appendix). The high frequency limit polarizabilities $m_z(\omega{=}\infty)$ and $m_t(\omega{=}\infty)$ for a conducting spheroid are given by the same formulae with permeability artificially set to zero (e.g., Silvester and Omeragic, 1995). We approximate the transverse polarizability m_t using that of a sphere of the transverse diameter $2a' = 2a$. We approximate the axial polarizability m_z using the polarizability of a sphere of diameter $2b'$, where for prolate (elongated) spheroids

$$2b' \;=\; 2b \tag{1a}$$

the axial diameter, and for oblate (flattened) spheroids

$$b' \;=\; \left(\frac{b^2+ab}{2}\right)^{1/2}. \tag{1b}$$

In the frequency domain, we use the scaling

$$\begin{aligned} m_z(\omega) \;&\approx\; m_z(\omega{=}0) \\ &+\; \upsilon_z \left(m_{sphere(b')}(\omega) - m_{sphere(b')}(\omega{=}0) \right), \end{aligned} \tag{2}$$

$$\begin{aligned} m_t(\omega) \;&\approx\; m_t(\omega{=}0) \\ &+\; \upsilon_t \left(m_{sphere(a')}(\omega) - m_{sphere(a')}(\omega{=}0) \right), \end{aligned}$$

where

$$\upsilon_z \equiv \frac{m_z(\omega{=}\infty) - m_z(\omega{=}0)}{m_{sphere(b')}(\omega{=}\infty) - m_{sphere(b')}(\omega{=}0)}, \tag{3}$$

$$\upsilon_t \;\equiv\; \frac{m_t(\omega{=}\infty) - m_t(\omega{=}0)}{m_{sphere(a')}(\omega{=}\infty) - m_{sphere(a')}(\omega{=}0)}.$$

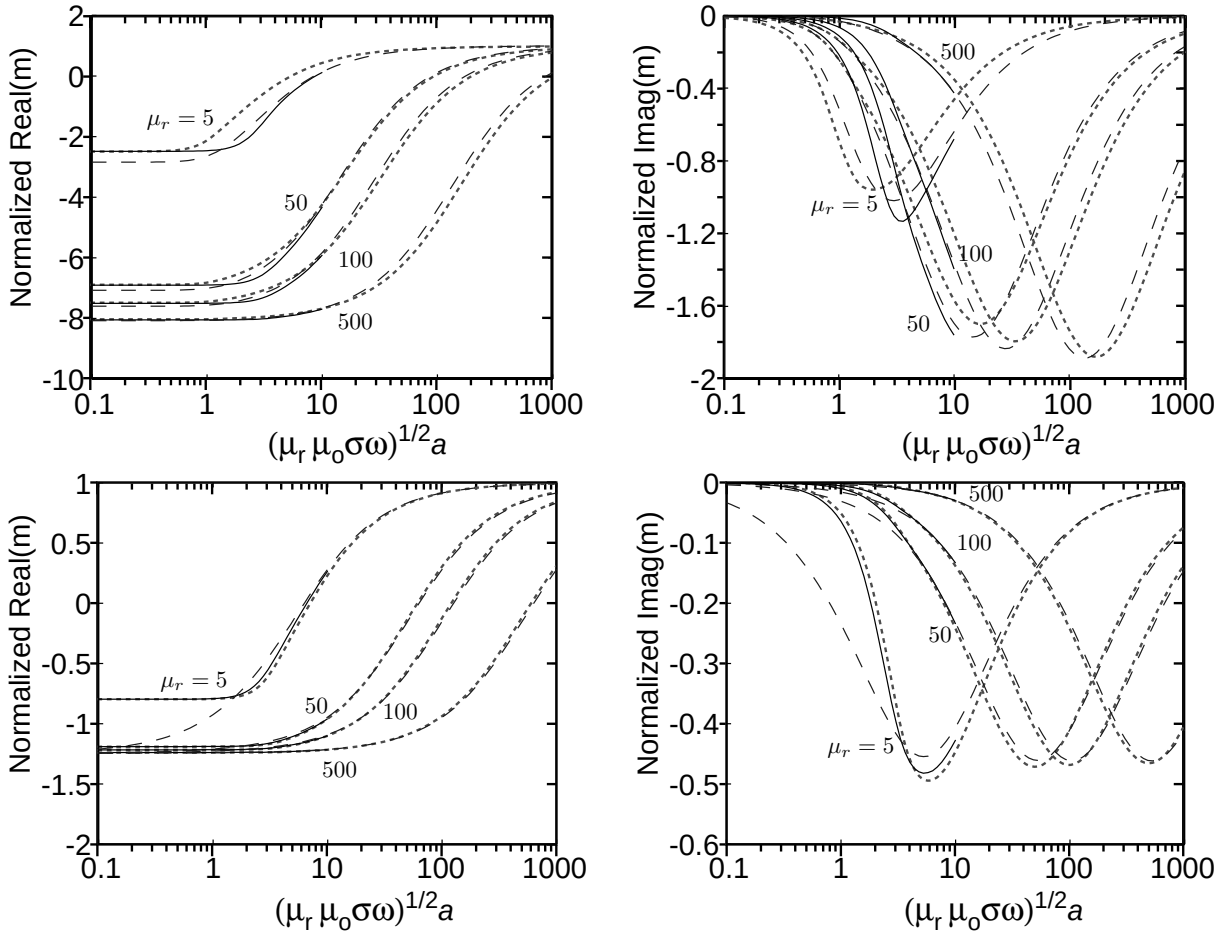

Figure 1: Dipole polarizability as a function of transverse induction number, normalized by high frequency limit $m(\omega{=}\infty)$, for 3:1 prolate spheroids of varying relative permeabilities μ_r. Upper; Axial excitation. Lower; Transverse excitation. Dotted; scaled sphere approximation (equations 2). Dashed; Ao, *et al.* SPD approximation. Solid; full spheroidal vector wavefunction solution.

This assures agreement of $m_z(\omega)$ and $m_t(\omega)$ with their limiting values at $\omega = 0$ and $\omega = \infty$. The rescaling is simpler in the time domain ;

$$m_z(t) \approx \upsilon_z m_{sphere(b')}(t)\,, \qquad (4)$$

$$m_t(t) \approx \upsilon_t m_{sphere(a')}(t),$$

for $t > 0$, as behaviour at $t > 0$ is unaffected by addition of constants in the frequency domain. Constants υ_z and υ_t depend only on aspect ratio and relative permeability, and, for large μ_r, only weakly on relative permeability. They are given explicitly in Appendix.

COMPARISON WITH PREVIOUS RESULTS

Frequency domain results for a prolate spheroid with aspect ratio b/a = 3 are plotted in Figure (1) (dotted) for relative permeabilities between 5 and 500, as a function of transverse induction number $(\mu_r \mu_o \sigma\omega)^{1/2}a$, where σ is the spheroid conductivity, and μ_o is the permeability of free space. Also shown are full solution results (solid) from Ao *et al.* (2001) for the frequencies for which they are calculable, and their high frequency (SPA) results. Agreement is better for transverse external fields, than for axial magnetic fields, and appears better in real parts than imaginary parts where amplitudes are smaller. Agreement is reasonable for $\mu_r \geq 50$. Similar results, varying aspect ratio b/a between 1 and 10 are

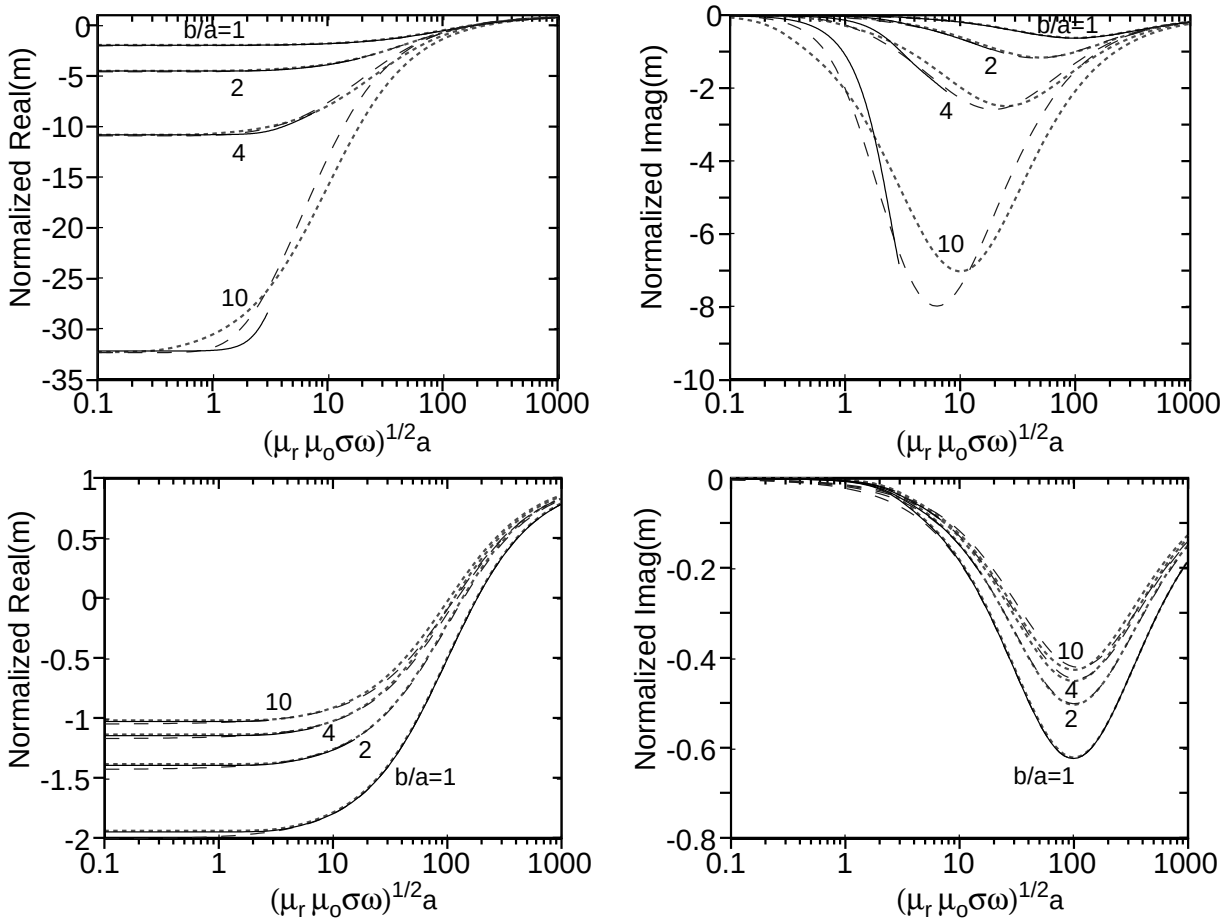

Figure 2: Dipole polarizability as a function of transverse induction number, normalized by high frequency limit $m(\omega{=}\infty)$, for prolate spheroids of varying elongation b/a, with relative permeability $\mu_r = 100$. Upper; Axial excitation. Lower; Transverse excitation. Dotted; scaled sphere approximation (equations 2). Dashed; Ao, *et al.* SPD approximation. Solid; full spheroidal vector wavefunction solution.

shown in Figure (2) (dotted) for prolate spheroids with relative permeability $\mu_r = 100$. Again, agreement is better for transverse external fields, than for axial external fields, and is better in real parts where amplitudes are larger than in the imaginary parts. Agreement is reasonable for elongations $b/a \leq 4$.

For a 3:1 prolate spheroid made of steel ($\sigma = 10^7 \Omega^{-1}$m, $\mu_r = 180$), the sphere response scaling constants are υ_z = 0.246, υ_t = 2.71. Time domain results for a 37 mm by 111 mm steel prolate spheroid are shown in Figure (3), for excitation by a step function turn-off primary field. For comparison, inverse Fourier transformed high frequency SPA results are also plotted, showing reasonable agreement. The discrepancies between the SPA approximation and the scaled sphere approximation for the transverse response after 0.04 s arise from the lack of a final exponential cut-out in the SPA results. Similar discrepancies are observed between SPA results and full analytic results for high permeability spheres (not shown) at times greater than the sphere's fundamental time constant ($\tau = \mu_o \mu_r \sigma a^2/d^2$, $d \approx 1.422\pi$).

In Figure (5) we compare approximation (2) with SPA results for oblate spheroids of varying aspect ratios and relative permeability m_r = 100. For oblate spheroids approximation using sphere results is reasonable for aspect ratios up to a/b = 4. A second example of time domain results is shown in Figure (4), for a 111 mm by 37 mm steel oblate spheroid

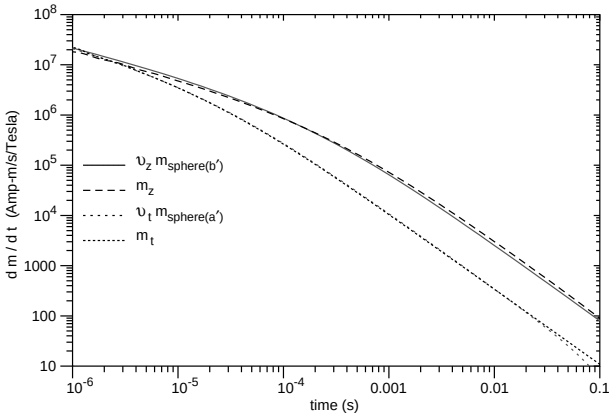

Figure 3: Dipole polarizability decay rate as a function of time, for a 37 mm by 111 mm steel prolate spheroid ($\sigma = 10^7\ \Omega^{-1}$m, $\mu_r = 180$), with step function turn-off excitation. Solid; scaled sphere approximation (equation 2a) for axial excitation. Long dash; Ao, *et al.* SPD approximation for axial excitation. Medium dash; scaled sphere approximation (equation 2b) for transverse excitation. Short dash; Ao, *et al.* SPD approximation for transverse excitation.

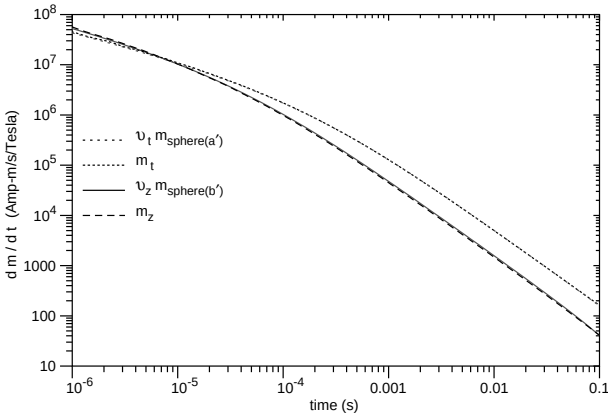

Figure 4: Dipole polarizability decay rate as a function of time, for a 111 mm by 37 mm steel oblate spheroid ($\sigma = 10^7\ \Omega^{-1}$m, $\mu_r = 180$), with step function turn-off excitation. Solid; scaled sphere approximation (equation 2a) for axial excitation. Long dash; Ao, *et al.* SPD approximation for axial excitation. Medium dash; scaled sphere approximation (equation 2b) for transverse excitation. Short dash; Ao, *et al.* SPD approximation for transverse excitation.

(scaling constants υ_z = 3.08, υ_t = 0.490) for excitation by a step function turn-off primary field. Inverse Fourier transformed high frequency SPA results are also plotted. Scaled sphere and SPA results are nearly indistinguishable.

Both SPA approximation and scaled sphere approximation predict a cross over between axial and transverse polarizability decay rates for the oblate spheroid at about 10 μs, and at about 1 μs for the prolate spheroid. After cross over, the two become easily distinguishable; both have a greater polarizability decay rate in their longer direction. In plots of an object's inductive response, time scales with object scale squared. So, for spheroids of the same conductivity, permeability and aspect ratios, but two times larger in dimension, the cross over points occur 4 times later.

CONCLUSION

For high permeability conductive spheroids of moderate aspect ratio, the inductive response of spheroids is reasonably well modelled by spheres of the appropriate diameter (axial, transverse, or intermediate), with rescaling based on the differing volumes and D.C. magnetizations of the spheres and modelled spheroids. This simple model for spheroid response makes understanding spheroid responses easier, and makes analysis of detector bandwidth requirements simpler. In as much as the spheroid responses are faithfully reproduced by the scaled sphere responses, it follows that to be able to estimate the parameters affecting the shape of the spheroid responses, one must be able to estimate the parameters affecting the shape of the sphere response, namely sphere radius, conductivity and permeability. Given the very simple relationship between sphere responses and spheroid responses, the effects of changing permeability and conductivity on the shape of spheroid responses are identical to their effects on the shape of sphere responses. As the magnitude of variations of spheroid responses with frequency or time differs by factors (3) from sphere responses, the noise levels needed to resolve spheroid attributes differ from the noise levels needed to resolve sphere attributes by these same

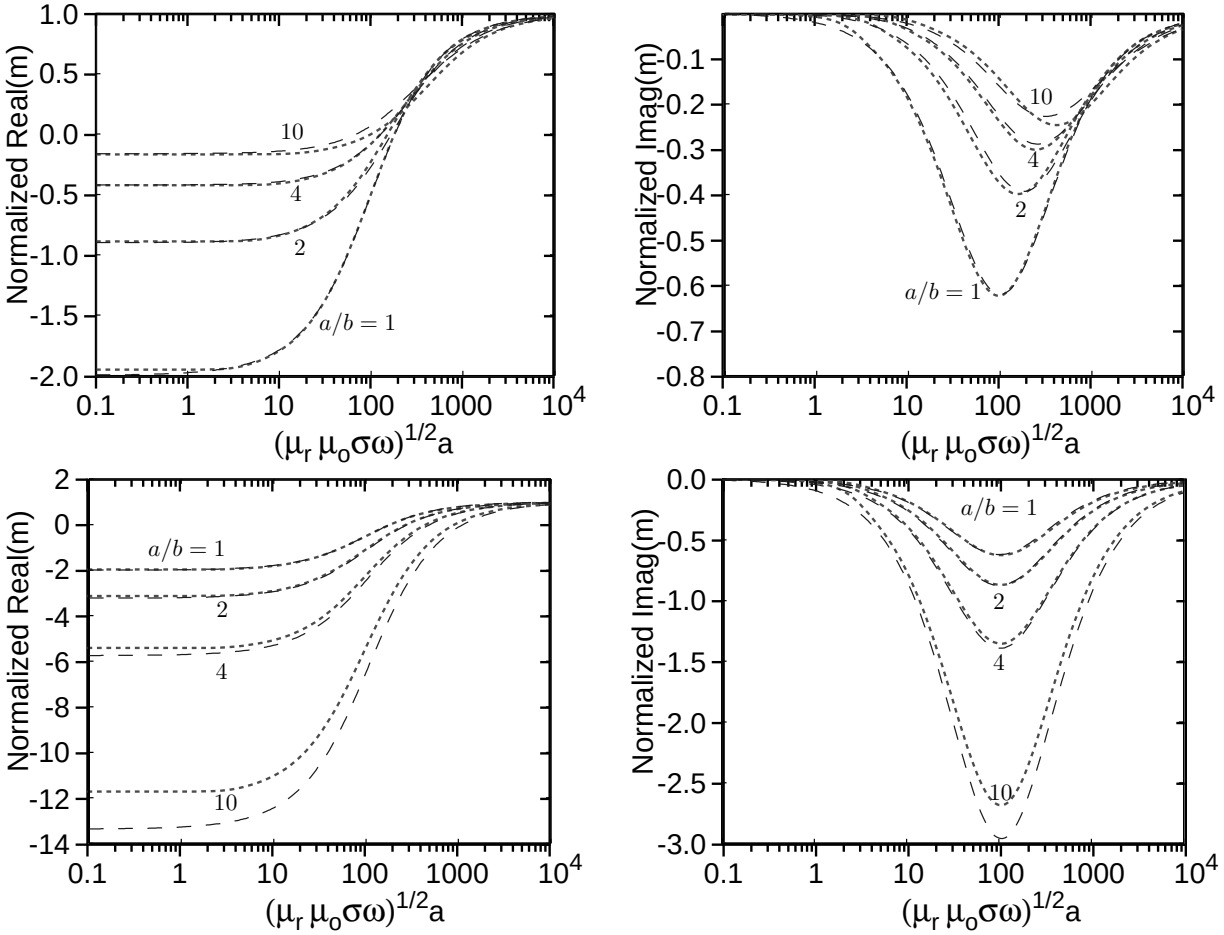

Figure 5: Dipole polarizability as a function of transverse induction number, normalized by high frequency limit $m(\omega{=}\infty)$, for oblate spheroids of varying flatness a/b, with relative permeability $\mu_r = 100$. Upper; Axial excitation. Lower; Transverse excitation. Dotted; scaled sphere approximation (equations 2). Dashed; Ao, *et al.* SPD approximation.

factors. However, the frequency bands or time windows needed to resolve a spheroid's attributes σ, μ_r, and b or a, are evidently the same as for spheres of the corresponding diameters.

ACKNOWLEDGEMENTS

The authors are grateful to K. O'Neill for providing Fortran code for computing the high frequency approximation of Ao *et al.*, and for assorted preprints. This work was supported by the US Department of the Army contract No. W74RDV93447299, under the auspices of the Strategic Environmental Research and Development Program (SERDP).

APPENDIX: SPHEROID FREQUENCY LIMITS

In the low frequency limit ($\omega = 0$) the magnetization is constant inside a spheroid. Following Silvester and Omeragic (1995), for axial magnetic field H_z, the magnetization inside the spheroid is given by

$$M_z(\omega{=}0) = \frac{\mu_r - 1}{1 + A_z(\mu_r - 1)} H_z, \qquad (\text{A}{-}1\text{a})$$

and for transverse magnetic field H_t,

$$M_t(\omega{=}0) = \frac{\mu_r - 1}{1 + A_t(\mu_r - 1)} H_t, \qquad (\text{A}{-}1\text{b})$$

where A_z and A_t are known as depolarization coefficients. For prolate spheroids, with reciprocal elon-

gation $\rho = a/b < 1$;

$$A_z = \frac{\rho^2}{1-\rho^2}\left[\frac{\text{arctanh}\sqrt{1-\rho^2}}{(1-\rho^2)^{1/2}} - 1\right], \quad \text{(A-2)}$$

$$A_t = \frac{1}{2(1-\rho^2)}\left[1 - \frac{\rho^2\text{arctanh}\sqrt{1-\rho^2}}{(1-\rho^2)^{1/2}}\right].$$

For relevant arguments, $\text{arctanh}(x) = \log((1+x)/(1-x))\ /2$, $(0 \le x^2 < 1)$. For oblate spheroids, $\rho = a/b > 1$, and

$$A_z = \frac{\rho^2}{\rho^2-1}\left[1 - \frac{\arctan\sqrt{\rho^2-1}}{(\rho^2-1)^{1/2}}\right], \quad \text{(A-3)}$$

$$A_t = \frac{1}{2(\rho^2-1)}\left[\frac{\rho^2\arctan\sqrt{\rho^2-1}}{(\rho^2-1)^{1/2}} - 1\right].$$

For spheres $\rho \to 1$ and $A_z \to A_t \to 1/3$. High frequency limit equivalent magnetizations $M_z(\omega{=}\infty)$ and $M_t(\omega{=}\infty)$ are given by equations (A-1) with relative permeability μ_r set to zero.

The magnetic dipole moment is given by the product of the magnetization and volume, $M_z\, V_{spheroid}$ or $M_t\, V_{spheroid}$, and the polarizability by the ratio of dipole moment to external magnetic field $\mu_o H$;

$$m_z(\omega{=}0) = \frac{\mu_r - 1}{1 + A_z(\mu_r - 1)} V_{spheroid}/\mu_o\,, \quad \text{(A-4)}$$

$$m_t(\omega{=}0) = \frac{\mu_r - 1}{1 + A_t(\mu_r - 1)} V_{spheroid}/\mu_o\,,$$

where $V_{spheroid} = 4\pi a^2 b/3$. High frequency limit polarizabilities $m_z(\omega{=}\infty)$ and $m_t(\omega{=}\infty)$ are obtained setting $\mu_r = 0$ in equations (A-4). Thus, relations (3) work out to

$$\upsilon_z = \frac{2}{9}\frac{a^2 b}{b'^3}\frac{(\mu_r+2)}{\mu_r}\left[\frac{1}{1-A_z} + \frac{\mu_r - 1}{1 + A_z(\mu_r - 1)}\right], \quad \text{(A-5)}$$

$$\upsilon_t = \frac{2}{9}\frac{a^2 b}{a'^3}\frac{(\mu_r+2)}{\mu_r}\left[\frac{1}{1-A_t} + \frac{\mu_r - 1}{1 + A_t(\mu_r - 1)}\right].$$

REFERENCES

C. O. Ao, H. Braunisch, K. O'Neill, J. A. Kong, L. Tsang, and J. T. Johnson, Broadband electromagnetic induction response from conducting and permeable spheroids, Proc. S.P.I.E, vol. 4394: Detection and Remediation Technologies for Mines and Minelike Targets VI, Orlando, April 2001.

P. Silvester, and D. Omeragic, Sensitivity of metal detectors to spheroidal targets, *IEEE Trans. Geosci. Remote Sensing*, vol. 33, no. 6, 1331-1335, 1995.